Published in final edited form as:
Chemistry. 2012 January 23; 18(4): 1084–1093. doi:10.1002/chem.201103215.

Electron-Transfer Reduction of Dinuclear Copper Peroxo and Bis-μ-oxo Complexes Leading to the Catalytic Four-Electron Reduction of Dioxygen to Water

Laleh Tahsini[a], **Hiroaki Kotani**[b], **Yong-Min Lee**[a], **Jaeheung Cho**[a], **Wonwoo Nam**[a], **Kenneth D. Karlin**[a,c], and **Shunichi Fukuzumi**[a,b]

Wonwoo Nam: wwnam@ewha.ac.kr; Kenneth D. Karlin: karlin@jhu.edu; Shunichi Fukuzumi: fukuzumi@chem.eng.osaka-u.ac.jp

[a]Department of Bioinspired Science, Ewha Womans University, Seoul 120-750 (Korea)

[b]Department of Material and Life Science, Graduate School of Engineering, Osaka University, ALCA (Japan) Science and Technology Agency (JST), Suita, Osaka 565-0871 (Japan), Fax: (+81)-6-6879-7368

[c]Department of Chemistry, Johns Hopkins University, Baltimore, Maryland 21218 (USA)

Abstract

The four-electron reduction of dioxygen by decamethylferrocene (Fc*) to water is efficiently catalyzed by a binuclear copper(II) complex (**1**) and a mononuclear copper(II) complex (**2**) in the presence of trifluoroacetic acid in acetone at 298 K. Fast electron transfer from Fc* to **1** and **2** affords the corresponding Cu^{I} complexes, which react at low temperature (193 K) with dioxygen to afford the η^2:η^2-peroxo dicopper(II) (**3**) and bis-μ-oxo dicopper(III) (**4**) intermediates, respectively. The rate constants for electron transfer from Fc* and octamethylferrocene (Me_8Fc) to **1** as well as electron transfer from Fc* and Me_8Fc to **3** were determined at various temperatures, leading to activation enthalpies and entropies. The activation entropies of electron transfer from Fc* and Me_8Fc to **1** were determined to be close to zero, as expected for outer-sphere electron-transfer reactions without formation of any intermediates. For electron transfer from Fc* and Me_8Fc to **3**, the activation entropies were also found to be close to zero. Such agreement indicates that the η^2:η^2-peroxo complex (**3**) is directly reduced by Fc* rather than via the conversion to the corresponding bis-μ-oxo complex, followed by the electron-transfer reduction by Fc* leading to the four-electron reduction of dioxygen to water. The bis-μ-oxo species (**4**) is reduced by Fc* with a much faster rate than the η^2:η^2-peroxo complex (**3**), but this also leads to the four-electron reduction of dioxygen to water.

Keywords

copper; dioxygen; electron transfer; ferrocene; oxygen reduction reaction

Correspondence to: Wonwoo Nam, wwnam@ewha.ac.kr; Kenneth D. Karlin, karlin@jhu.edu; Shunichi Fukuzumi, fukuzumi@chem.eng.osaka-u.ac.jp.

Supporting information for this article is available on the WWW under http://dx.doi.org/10.1002/chem.201103215.

Introduction

Cytochrome *c* oxidases (C*c*Os), with a bimetallic active site consisting of a heme *a* and Cu (Fe_{a3}/Cu_B) are capable of catalyzing the four-electron reduction of dioxygen to water.[1, 2] Multicopper oxidases, such as laccase, can also activate dioxygen at a site containing a three-plus-one arrangement of four Cu atoms.[3–5] Extensive efforts have been devoted to develop efficient catalysts for the four-electron reduction of dioxygen because of its great biological interest[6–13] as well as technological significance, for example, in fuel cells.[14–18] Electrocatalytic reduction of dioxygen has frequently been used to probe the catalytic reactivity of synthetic C*c*O model complexes[14–16] and copper complexes by themselves have been reported to exhibit electroactivity for the four-electron reduction of dioxygen.[18] In contrast to such heterogeneous systems, investigations on the catalytic reduction of dioxygen by metal complexes in homogeneous systems have provided deeper insight into the catalytic mechanism of the four-electron reduction of dioxygen by detecting reactive metal–dioxygen intermediates as well as by the information provided from detailed kinetics studies.[10–12, 13a,b]

With regard to copper–dioxygen intermediates, η^2:η^2-peroxo and bis-μ-oxo species have been extensively studied in reactions of low-valent metal complexes and dioxygen.[19–24] However, even if the reaction of an η^2:η^2-peroxo species with a substrate (pathway a in Scheme 1) is followed, the reaction may undergo the conversion via the bis-μ-oxo species, which may be much more reactive than the corresponding η^2:η^2-peroxo species (pathway b in Scheme 1). Thus, it has always been very difficult to clarify the actual reactive intermediate, which could be either the peroxo (pathway a in Scheme 1) or bis-μ-oxo species (pathway b in Scheme 1) in the reactions with substrates, unless the rate-determining step is the interconversion between them when the rate would be independent of concentrations of substrates.[19–24] In these regards, the roles of the η^2:η^2-peroxo versus bis-μ-oxo species in the catalytic four-electron reduction of O_2 have yet to be established. There has so far been no report on electron-transfer reactions of η^2:η^2-peroxo and bis-μ-oxo dicopper species.

We report herein that a binuclear copper complex, $[Cu^{II}_2(N3)(H_2O)_2](ClO_4)_4$ (**1**; N3 = (−$(CH_2)_3$-linked bis[2-(2-pyridyl)ethyl]amine),[25] and a mononuclear copper complex, $[Cu^{II}(BzPY1)(EtOH)](ClO_4)_2$ (**2**; BzPY1 = *N*,*N*-bis[2-(2-pyridyl)-ethyl]benzylamine),[26] efficiently catalyze the four-electron reduction of O_2 by decamethylferrocene (Fc*) in the presence of trifluoroacetic acid (TFA) in acetone at 298 K. The spectroscopic detection of the intermediate and the dynamics reveal that the catalytic four-electron reduction of O_2 by Fc* with **1** occurs through electron transfer from Fc* to **1**, followed by the reaction of the resulting dicopper(I) complex with O_2 to afford a η^2:η^2-peroxo intermediate (**3**), which is further reduced by electron transfer from Fc*. Alternatively a possible interconversion to a bis-μ-oxo dicopper(III) species may occur, followed by fast electron-transfer reduction by Fc*. Electron-transfer reactions of ferrocene derivatives are known to occur by means of an outer-sphere pathway, in which the activation entropy is close to zero.[27] If electron transfer from ferrocene derivatives to **3** proceeds directly by pathway a in Scheme 1, the activation entropy should be the same as electron transfer from ferrocene derivatives to **1**. Thus, comparison of the activation entropies of electron transfer from ferrocene derivatives to **3** with those of the electron transfer to **1** provides a unique opportunity to distinguish between pathways a and b in Scheme 1. In the case of $[Cu^{II}(BzPY1)(EtOH)](ClO_4)_2$ (**2**), the catalytic four-electron reduction of O_2 by Fc* comes about by reduction of **2**, followed by the reaction of the resulting Cu^I complex with O_2 to afford a bis-μ-oxo dicopper(III) species, which here is in fact the key intermediate, reduced by fast electron transfer from Fc*.

Results and Discussion

Synthesis and structure of the binuclear Cu^{II} complex

The complex $[Cu^{II}_2(N3)(H_2O)_2](ClO_4)_4$ (**1**) was prepared by the reaction of $Cu^{II}(ClO_4)_2 \cdot 6H_2O$ with the N3 ligand in acetone and recrystallized from acetone/diethyl ether. The X-ray crystal structure is shown in Figure 1, in which the copper coordination units are separated from each other with Cu···Cu = 7.268(2) Å. The Cu^{II} ions are found to be the pseudotetrahedral geometry coordinated to two pyridyl and one amino nitrogen atoms from the tridentate chelate as reported for the dicopper(I) complex[25b] (for crystal data, structure refinements and bond lengths, see Tables S1 and S2 in Supporting Information).

The large Cu···Cu distance resulted in no paramagnetic coupling, as evidenced in the EPR spectrum of **1** (Figure 2). The $A_{\|}$ value is expected to decrease as the degree of geometrical distortion increases from a square-planar structure towards a tetrahedral structure.[28, 29] Thus, the observed small $A_{\|}$ value (62 G) of **1** in acetone (Figure 2) indicates that the pseudotetrahedral geometry in Figure 1 is kept in solution. In contrast to the EPR spectrum of **1**, the $A_{\|}$ value (170 G) of **2** (Figure 2) indicates much less distortion from planarity. Such a structural difference between **1** and **2** is expected to affect the electron-transfer properties (vide infra). In both cases, the EPR spectra in Figure 2 are axial with $g_{\|} > g_{\perp} > 2.0$, indicating a $d_{x^2-y^2}$ ground state.[30]

Redox potentials of Cu^{II} complexes

Cyclic voltammograms of **1** and **2** in deaerated acetone containing $TBAPF_6$ (0.10 M; $TBAPF_6$ = tetrabutylammonium hexafluorophosphate) at 298 K are shown in Figure 3. In each case, a quasi-reversible couple between the Cu^{II} and Cu^{I} complexes is observed. From the $E_{1/2}$ values, the one-electron reduction potentials (E_{red}) of **1** and **2** were determined to be 0.37 and 0.11 V (vs. SCE), respectively. Thus, when Fc* (E_{ox} = −0.08 V vs. SCE)[31, 32] and octamethylferrocene (Me_8Fc: E_{ox} = −0.04 V vs. SCE)[31, 32] are employed as electron donors, electron transfer from Fc* and Me_8Fc to **1** and **2** occurs to produce the corresponding ferrocenium cations and the Cu^{I} complexes.

The larger peak separation between cathodic and anodic peaks of **2** than those of **1** at the same sweep rate in Figure 3 (for example, 0.16 V for **1** and 0.19 V for **2** at the scan rate of 0.10 V s^{-1}) is consistent with the larger structural change expected for **2** as compared with **1**. A more quantitative analysis was performed by analyzing the rates of electron transfer from ferrocene derivatives to **1** and **2** (vide infra).

Catalytic four-electron reduction of dioxygen by Fc*

The addition of a catalytic amount of **1** or **2** to an O_2-saturated acetone solution of Fc* and trifluoroacetic acid (TFA) results in the efficient reduction of O_2 by Fc* to afford the corresponding ferrocenium cation (Fc^{*+}). Figure 4 shows the spectral changes for the catalytic reduction of O_2 by Fc* with **1** and **2** in the presence of TFA in acetone at 298 K.

When more than four equivalents of Fc* relative to O_2 (that is, limiting [O_2]) were employed, four equivalents of Fc^{*+} (λ_{max} = 780 nm) were formed in the presence of excess TFA (Figure 4).[33] Although, O_2 slowly oxidizes Fc* without the presence of catalyst with a large excess of TFA in acetone, there was no further oxidation of Fc* under the present experimental conditions, see the inset of Figure 4.[34] Iodometric titration experiments (see Figure S1 in the Supporting Information)[35] confirmed that no H_2O_2 was formed. Thus, the four-electron reduction of O_2 by Fc* occurs efficiently with catalytic amounts of **1** or **2** in the presence of TFA [Eq. (1)]. When Fc* was replaced by octamethylferrocene (Me_8Fc), the

four-electron reduction of O_2 by Fc* also occurred efficiently with **1**. However, no catalytic reduction of O_2 with **1** occurred when Fc* was replaced by 1,1'-dimethylferrocene (Me_2Fc).

$$O_2 + 4\,Fc^{*} + 4\,H^{+} \rightarrow 4\,Fc^{*+} + 2\,H_2O \quad (1)$$

Catalytic mechanisms of four-electron reduction of dioxygen by Fc*

The catalytic mechanisms of the four-electron reduction of O_2 by Fc* with **1** and **2** were examined step by step. First, electron transfer from Fc* to **1** and **2** was examined by stopped flow measurements. Electron transfer from Fc* (E_{ox} = −0.08 V vs. SCE) to **1** (E_{red} = 0.37 V vs. SCE) and **2** (E_{red} = 0.11 V vs. SCE) (Figure 3) occurs efficiently because the reactions are exergonic ($\Delta G_{et} < 0$). The rate of electron transfer from Fc* to **1** was too fast to be determined by stopped flow measurements in acetone at 298 K. When Fc* is replaced by weaker electron donors (1,1'-dimethylferrocene Me_2Fc: E_{ox} = 0.26 V vs. SCE and ferrocene Fc: E_{ox} = 0.37 V vs. SCE)[31, 32], the rates of formation of ferrocenium cations could then be readily determined. The rates obeyed clean pseudo-first-order kinetics as shown in Figure 5 A. This indicates that electron transfer from the ferrocene derivatives to **1** and **2** occurs directly without involvement of any rate-determining geometry change of the Cu^{II} complexes to a more active form, followed by rapid electron transfer. The second-order rate constants (k_{et1}) of electron transfer from ferrocene derivatives to **1** and **2** were determined from the slopes of linear plots of the pseudo-first-order rate constants versus concentrations of ferrocene derivatives (Figure 5 B). The k_{et1} values for electron transfer are listed in Table 1.

According to the Marcus theory of electron transfer, the k_{et} value is determined by the free energy change of electron transfer (ΔG_{et}) and the reorganization energy of electron transfer in Equation (2) in which Z is the collision frequency taken as 1×10^{11} $_{M}^{-1}$ s^{-1}.[36]

$$k_{et} = Z\exp[-(\lambda/4)(1+\Delta G_{et}/\lambda)^2/RT] \quad (2)$$

The ΔG_{et} values of electron transfer from ferrocene derivatives to Cu^{II} complexes (**1** and **2**) are obtained from the E_{ox} values of ferrocene derivatives (Table 1) and the E_{red} values of Cu^{II} complexes (Figure 3). Then, the λ value of electron transfer from is determined from the k_{et} and ΔG_{et} values using Equation (3), which is derived from Equation (2).[37]

$$\lambda = -\Delta G_{et} - 2RT\ln(k_{et}/Z) + [\{\Delta G_{et} + 2RT\ln(k_{et}/Z)\}^2 - (\Delta G_{et})^2]^{1/2} \quad (3)$$

Virtually the same λ value (1.6 eV) is obtained from the k_{et} and ΔG_{et} values of electron transfer from Me_2Fc and Fc to **1** by using Equation 3. On the other hand, a significantly larger λ value (2.1 eV) is obtained from the k_{et} and ΔG_{et} values of electron transfer from Fc* and Me_8Fc to **2** by using Equation 3. Because the λ values of electron self-exchange between ferrocene derivatives and the corresponding ferrocenium cation derivatives are nearly the same irrespective of the number of methyl substituent,[38] the smaller λ value of the electron-transfer reduction of **1** relative to **2** results from the pseudotetrahedral structure of **1** (Figure 1), which minimizes the structural change upon the electron-transfer reduction.

Once complex **1** is reduced to the Cu^{I} complex $[Cu^{I}_2(N_3)]^{2+}$, the reaction with O_2 is known to afford the η^2:η^2-peroxo complex **3** [Eq. (4); Scheme 2 where L is a solvent].[25b]

$$[Cu^{I}_2(N3)]^{2+} + O_2 \rightarrow [Cu^{II}_2(N3)(O_2)]^{2+} \quad (4)$$

Electron transfer from Fc* to **3** occurs to produce two equivalents of Fc^{*+} in acetone at 193 K [Eq. (5)] as shown in Figure 6; the decay of absorbance at 490 nm due to **3** is accompanied by the appearance of absorbance at 780 nm due to Fc^{*+} (inset of Figure 6).

$$[Cu^{II}{}_2(N3)(O_2)]^{2+} + 2Fc^{*} \rightarrow [Cu^{II}{}_2(N3)(O)_2] + 2Fc^{*+} \quad (5)$$

The one-step reaction in Figure 6 suggests that initial electron transfer from Fc* to **3** is the rate-determining step followed by rapid electron transfer from Fc* to $[Cu^{II}{}_2(N3)(O_2)]^{+}$. The rate of electron transfer from Fc* to **3** also obeyed clean pseudo-first-order kinetics (Figure 7 A) and the pseudo-first-order rate constant (k_{obs}) increases linearly with increasing concentration of Fc* (Figure 7 B). The second-order rate constant (k_{et2}) of electron transfer from Fc* to **3** was determined from the slope of a linear plot of k_{obs} vs. [Fc*] to be 18 $_{M}{}^{-1}$ s^{-1} at 193 K. The rate of electron transfer from Fc* to **3** was not affected by the presence of one equivalent of TFA (see Figure S2 in the Supporting Information). This indicates the electron transfer is not coupled with the protonation of **3**.[39] When Fc* was replaced by a weaker electron donor (Me_2Fc), no electron transfer from Me_2Fc to **3** occurred at 193 K although electron transfer from Me_2Fc to **1** occurred efficiently. This may be the reason why no catalytic reduction of O_2 by Me_2Fc occurred.

When Me_2Fc is replaced by *N,N,N',N'*-tetramethylphenylene-diamine (TMPD), electron transfer from TMPD to **3** occurred to completion as indicated by disappearance of the absorption band at 490 nm due to **3**, which was accompanied by appearance of the absorption band at 600 nm due to $TMPD^{\cdot+}$ (Figure S4 in SI).[40] Based on the one-electron oxidation potentials of TMPD (E_{ox} = 0.12 V vs. SCE)[40b] and Me_2Fc (E_{ox} = 0.26 V vs. SCE),[31, 32] the one-electron reduction potential of **3** can be estimated to be E_{red} = (0.19 ± 0.07) V vs. SCE, which is significantly lower than the E_{red} value of **1** (0.37 V vs. SCE).

The temperature dependence of both the k_{et1} and k_{et2} values was examined at low temperatures. The Eyring plots of k_{et1} and k_{et2} shown in Figure 8 afforded the activation parameters that are listed in Table 2. If electron transfer from Fc* and Me_8Fc to **3** occurred via the conversion to the putative isomeric bis-μ-oxo intermediate ($[Cu^{III}{}_2(N3)(O)_2]^{2+}$), the observed rate constant (k_{obs}) would be given by Equation (6) in which K_o describes the equilibrium between $[Cu^{II}{}_2(N3)(O_2)]^{2+}$ (**3**) and $[Cu^{III}{}_2(N3)(O)_2]^{2+}$ in Scheme 3.

$$k_{obs} = k_{et} K_o \quad (6)$$

The K_o value should be much smaller than 1 ($K_o \ll 1$), because no bis-μ-oxo intermediate has been observed.[41] In such a case, the observed rate constant (k_{obs}) would be much smaller than the rate constant of electron transfer to the putative bis-μ-oxo intermediate ($k_{obs} \ll k_{et}$) and the observed activation entropy would not be the same as that of electron transfer, because it would be given as the sum of the activation entropy of electron transfer ($\Delta S_{et}^{\ddagger} \approx 0$) and the entropy of the formation of the bis-μ-oxo intermediate ($\Delta S_o < 0$), $\Delta S_{obs}^{\ddagger} = \Delta S_{et}^{\ddagger} + \Delta S_o$ (< 0).[42] Virtually the same $\Delta S^{\ddagger}$ values (ca. 0) for electron transfer from Fc* and Me_8Fc to **1** and **3** given in Table 2 clearly indicate that electron transfer from Fc* and Me_8Fc to **3** occurs directly rather than through the interconversion from **3** to the corresponding bis-μ-oxo intermediate followed by rapid electron transfer from Fc* and Me_8Fc (Scheme 3).

Because the E_{red} value of **3** was evaluated as (0.19 ± 0.07) V (vide supra), the ΔG_{et} values of electron transfer from Fc* and Me_8Fc were evaluated to be (−0.27 ± 0.07) and (−0.23 ± 0.07) eV, respectively. The λ value of electron transfer from Fc* and Me_8Fc to **3** was estimated from the k_{et} and ΔG_{et} values by using Equation (3) to be (2.2 ± 0.1) eV, which is

significantly larger than the value of electron transfer from ferrocene derivatives to **1**. The larger λ value of **3** with respect to **1** is consistent with direct electron transfer from ferrocene derivatives to **3**, which involves the cleavage of the O–O bond.

The catalytic mechanism of the possible two-electron versus the actual four-electron reduction of O_2 by Fc* with **1** is summarized in Scheme 4. The initial electron transfer from Fc* to **1** is fast, and it is followed by the reaction of the dicopper(I) complex with O_2 to afford the η^2:η^2-peroxo complex **3**. The efficient direct electron-transfer reduction of **3** by Fc* rather than that through the conversion of the η^2:η^2-peroxo complex **3** to the bis-μ-oxo complex, as compared with the formation of H_2O_2 by the reaction of **3** with protons, may be the rate-determining step, leading to the catalytic four-electron reduction of O_2 by Fc*.

When $[Cu^{II}(BzPY1)]^{2+}$ (**2**) is reduced to the Cu^I complex, the reaction with O_2 is known to afford the bis-μ-oxo complex **4** (Scheme 5).[16] The formation of **4** (λ_{max} = 390 nm) by the reaction of the Cu^I complex with O_2 is shown in Figure 9. Electron transfer from Fc* to **4** occurs rapidly upon mixing in acetone even at 193 K to produce two equivalents of Fc^{*+} (Figure 9) and the rate was not affected by TFA. The same immediate reaction occurs with the weaker electron donors such as Me_2Fc and Fc as well. In the case of **2**, no catalytic reduction of O_2 by Me_2Fc occurred, because the initial electron transfer from Me_2Fc to **2** is endergonic ($\Delta G_{et} > 0$) and thereby the catalytic cycle cannot be started.

Conclusion

In summary, copper complexes **1** and **2** act as efficient catalysts for the four-electron four-proton reduction of O_2 by Fc* in the presence of TFA in acetone. In the case of **1**, the direct electron-transfer reduction of the η^2:η^2-peroxo complex **3** by Fc* rather than through the interconversion from **3** to a bis-μ-oxo complex isomer occurs. For **2**, the rapid reduction of bis-μ-oxo intermediate (**4**) also results in the catalytic four-electron reduction of O_2 by Fc*. The present study broadens the range of copper complexes known to be effective in O_2 reduction chemistry, and in this context highlights ligand design which leads to varying O_2 adduct Cu_2O_2 structures. We have also for the first time clarified the roles of the η^2:η^2-peroxo and bis-μ-oxo intermediates in the catalytic four-electron reduction of O_2 to water.

Experimental Section

Materials

Commercially available reagents, decamethylferrocene (Fc*), octamethylferrocene (Me_8Fc), 1,1'-dimethylferrocene (Me_2Fc), ferrocene (Fc), trifluoroacetic acid (TFA), hydrogen peroxide (50%), and NaI (Junsei Chemical Co., Ltd.) were the best available purity and used without further purification unless otherwise stated. Acetone was dried according to the literature procedures[43] and distilled under Ar prior to use. Copper complexes, $[Cu^I_2(N3)(CH_3CN)_2](BArF)_2$ (BArF = tetrakis-(pentafluorophenyl) borate) [N3 = (−$(CH_2)_3$-linked bis[(2-(2-pyridyl)ethyl)-amine], $[Cu^I(BzPY1)(CH_3CN)]BArF$, and $[Cu^{II}(BzPY1)(EtOH)](ClO_4)_2$ (**2**: BzPY1 = *N*,*N*-bis[2-(2-pyridyl)ethyl]benzylamine) were prepared according to the literature procedures.[25b, 26]

Synthesis of $[Cu^{II}_2(N3)(H_2O)_2](ClO_4)_4$ (1)

A solution of N3 (0.075 g, 0.15 mmol) in acetone (2.0 mL) was added to a solution of $Cu(ClO_4)_2.6\,H_2O$ (0.112 g, 0.30 mmol) in acetone (3.0 mL) giving a deep blue solution. After stirring for an hour, the solution was filtered and layered with diethyl ether. The greenish blue crystals were separated and dried (yield, 85%). Suitable crystals for X-ray crystallography were obtained by recrystallization from acetone/Et_2O. Elemental analysis

calcd (%) for $C_{31}H_{42}N_6O_{18}Cl_4Cu_2\cdot(CH_3)_2CO$: C, 36.67; H, 4.34; N, 7.55; found: C, 36.18; H, 4.09; N, 7.37.

X-ray crystallography

A single crystal of **1**-$(ClO_4)_4\cdot CH_3COCH_3$, was picked from solutions by a nylon loop (Hampton Research Co.) on a hand made cooper plate mounted inside a liquid N_2 Dewar vessel at about 233 K and mounted on a goniometer head in an N_2 cryostream. Data collection was carried out on a Bruker SMART AXS diffractometer equipped with a monochromator in the $Mo_{K\alpha}$ (λ = 0.71073 Å) incident beam. The CCD data were integrated and scaled using the Bruker-SAINT software package, and the structure was solved and refined using SHEXTL V 6.12.[44] The crystal contains four perchlorate anions, two of which are disordered. Three oxygen atoms of the two disordered perchlorate anions were situated on a twofold axis. All non-hydrogen atoms were refined with anisotropic thermal parameters. Hydrogen atoms were located in the calculated positions. H atoms on the acetone molecule were not located. Crystal data for **1**-$(ClO_4)_4\cdot CH_3COCH_3$:$C_{17}H_{21}Cl_2CuN_3O_{9.5}$, orthorhombic, *Cmcm*, Z = 8, a = 13.8780(3), b = 11.8522(3), c = 26.8445(6) Å, V = 4415.51(18) $Å^3$, μ = 1.289 mm^{-1}, ρ_{calcd} = 1.666 g cm^{-3}, R_1 = 0.0529, wR_2 = 0.2162 for 2698 unique reflections, 179 variables. The crystallographic data for **1**-$(ClO_4)_4\cdot CH_3COCH_3$ are listed in Table S1 in the in the Supporting Information, and Table S2 lists the selected bond lengths and angles. CCDC-819947 (**1**-$(ClO_4)_4\cdot CH_3COCH_3$) contains the supplementary crystallographic data for this paper. These data can be obtained free of charge from The Cambridge Crystallographic Data Centre via www.ccdc.cam.ac.uk/data_request/cif.

Instrumentation

UV/Vis spectra were recorded on a Hewlett Packard 8453 diode array spectrophotometer equipped with a circulating water bath or an UNISOKU RSP-601 stopped-flow spectrometer equipped with a MOS-type highly sensitive photodiode array. Measurements of cyclic voltammetry (CV) were performed at 298 K using a CHI630B electrochemical analyzer in a deaerated acetone containing 0.10 M $TBAPF_6$ as a supporting electrolyte. A conventional three-electrode cell was used with a platinum working electrode and a platinum wire as a counter electrode. The measured potentials were recorded with respect to the Ag/Ag^+ (0.010 M). The redox potentials (vs. Ag/Ag^+) were converted to those vs. SCE by adding 0.29 V.[45] All electrochemical measurements were carried out under an Ar atmosphere.

UV/Vis spectral titration

The catalytic reduction of O_2 was observed by the spectral change in the presence of various concentrations of TFA at 298 K. Typically, a solution of TFA in dichloromethane (0–1.0 × 10^{-2} M) was added to an O_2-saturated acetone solution containing Fc* (2.0 × 10^{-3} M) and **1** or **2** (1.0 × 10^{-4} M). The concentration of the generated Fc^{*+} was determined from the absorption band at λ_{max} = 780 nm (ε = 5.8 × 10^2 M^{-1} cm^{-1}). The ε value of Fc^{*+} was confirmed by the electron-transfer oxidation of Fc* with *p*-benzoquinone in the presence of TFA. The limiting concentration of O_2 in an acetone solution was prepared by a mixed gas flow of O_2 and N_2. The mixed gas was controlled by using a gas mixer (Kofloc GB-3C, KOJIMA Instrument Inc.), which can mix two or more gases at a certain pressure and flow rate.

Iodometric titration for the determination of H_2O_2

The amount of H_2O_2 was determined by the titration by iodide ion. The diluted acetone solution (1/15) of the reduced product of O_2 was treated with an excess amount of NaI. The

amount of I_3^- formed was then determined by the visible spectrum (λ_{max} = 361 nm, ε = 2.5 × 10^4 $_M{}^{-1}$ cm^{-1}).

Kinetic measurements

Kinetic measurements at 298 K were performed on a UNISOKU RSP-601 stopped-flow spectrometer equipped with a MOS-type highly sensitive photodiode array or a Hewlett Packard 8453 photodiode-array spectrophotometer at 298 K. Kinetic measurements of electron transfer (ET) from Fc* and Me_8Fc to $[Cu^{II}_2(N3)(O_2)]^{2+}$ (**3**) to calculate thermodynamic parameters were performed using a Hewlett Packard Agilent 8453 photodiode-array spectrophotometer with a quartz cuvette (path length = 10 mm) at 193 K. Rates of electron transfer from Fc* to **1** or **2** were monitored by the rise of absorption bands due to Fc^{*+} and $[Cu^{II}_2(N3)(O_2)]^{2+}$ (**3**) or $[(BzPY1)Cu^{III}(O)_2Cu^{III}(BzPY1)]^{2+}$ (**4**). All kinetic measurements were carried out under pseudo-first-order conditions where concentrations of Fc* was maintained to be more than in tenfold excess compared to the concentration of **1** or **2**.

Acknowledgments

The research at EWU was supported by KRF/MEST of Korea through CRI, GRL (2010-00353) (to W.N.), WCU (R31-2008-000-10010-0) (to S.F., K.D.K. and W.N.), 2011 KRICT OASIS project (to W.N) and NRF (NRF-2010-1054-1-2) (to J.C.). K.D.K. also acknowledges the US National Institutes of Health (GM28962). This work at OU was supported by a Grant-in-Aid (20108010) and a Global COE program, “the Global Education and Research Center for Bio-Environmental Chemistry” from the Ministry of Education, Culture, Sports, Science and Technology, Japan (to S.F.).

References

1. a) Pereira MM, Santana M, Teixeira M. Biochim. Biophys. Acta Bioenrg. 2001; 1505:185.b) Ferguson-Miller S, Babcock GT. Chem. Rev. 1996; 96:2889. [PubMed: 11848844]
2. Yoshikawa S, Shinzawa-Itoh K, Nakashima R, Yaono R, Yamashita E, Inoue N, Yao M, Fei MJ, Libeu CP, Mizushima T, Yamaguchi H, Tomizaki T, Tsukihara T. Science. 1998; 280:1723. [PubMed: 9624044]
3. a) Messerschmidt, A. Multi-copper Oxidases. Singapore: Word Scientific; 1997. b) Riva S. Trends Biotechnol. 2006; 24:219. [PubMed: 16574262] c Rodgers CJ, Blanford CF, Giddens SR, Skamnioti P, Armstrong FA, Gurr SJ. Trends Biotechnol. 2010; 28:63. [PubMed: 19963293]
4. a) Solomon EI, Sundaram UM, Machonkin TE. Chem. Rev. 1996; 96:2563. [PubMed: 11848837] b) Solomon EI, Szilagyi RK, DeBeer George S, Basumallick L. Chem. Rev. 2004; 104:419. [PubMed: 14871131]
5. a) Yoon J, Mirica LM, Stack TDP, Solomon EI. J. Am. Chem. Soc. 2005; 127:13680. [PubMed: 16190734] b) Quintanar L, Yoon J, Aznar CP, Palmer AE, Andersson KK, Britt RD, Solomon EI. J. Am. Chem. Soc. 2005; 127:13832. [PubMed: 16201804]
6. a) Kim E, Chufán EE, Kamaraj K, Karlin KD. Chem. Rev. 2004; 104:1077. [PubMed: 14871150] b) Chufán EE, Puiu SC, Karlin KD. Acc. Chem. Res. 2007; 40:563. [PubMed: 17550225] c) Karlin KD, Kaderli S, Zuberbühler AD. Acc. Chem. Res. 1997; 30:139.
7. Que L Jr, Tolman WB. Angew. Chem. 2002; 114:1160. *Angew. Chem. Int. Ed.***2002**, *41*, 1114.
8. a) Blanford CF, Heath RS, Armstrong FA. Chem. Commun. 2007:1710.b) Mano N, Soukharev V, Heller A. J. Phys. Chem. B. 2006; 110:11180. [PubMed: 16771381]
9. a) Rywkin S, Hosten CM, Lombardi JR, Birke RL. Langmuir. 2002; 18:5869.b) Fukuzumi S, Kotani H, Lucas HR, Doi K, Suenobu T, Peterson RL, Karlin KD. J. Am. Chem. Soc. 2010; 132:6874. [PubMed: 20443560]
10. Halime Z, Kotani H, Fukuzumi S, Karlin KD. Proc. Natl. Acad. Sci. USA. 2011; 108:13990. [PubMed: 21808032]

11. a) Fukuzumi S, Mochizuki S, Tanaka T. Chem. Lett. 1989:27.b) Fukuzumi S, Mochizuki S, Tanaka T. J. Chem. Soc. Chem. Commun. 1989:391.c) Fukuzumi S, Mochizuki S, Tanaka T. Inorg. Chem. 1989; 28:2459.d) Fukuzumi S, Mochizuki S, Tanaka T. Inorg. Chem. 1990; 29:653.
12. a) Fukuzumi S, Okamoto K, Gros CP, Guilard R. J. Am. Chem. Soc. 2004; 126:10441. [PubMed: 15315460] b) Fukuzumi S, Okamoto K, Tokuda Y, Gros CP, Guilard R. J. Am. Chem. Soc. 2004; 126:17059. [PubMed: 15612745]
13. a) Rosenthal J, Nocera DG. Acc. Chem. Res. 2007; 40:543. [PubMed: 17595052] b) Rosenthal J, Nocera DG. Prog. Inorg. Chem. 2007; 55:483.c) Chang CJ, Loh Z-H, Shi C, Anson FC, Nocera DG. J. Am. Chem. Soc. 2004; 126:10013. [PubMed: 15303875]
14. a) Collman JP, Boulatov R, Sunderland CJ, Fu L. Chem. Rev. 2004; 104:561. [PubMed: 14871135] b) Collman, JP.; Boulatov, R.; Sunderland, CJ. The Porphyrin Handbook. Kadish, KM.; Smith, KM.; Guilard, R., editors. Vol. Vol. 11. Elsevier Science USA: 2003. p. 1-49.
15. a) Anson FC, Shi C, Steiger B. Acc. Chem. Res. 1997; 30:437.b) Shin H, Lee D-H, Kang C, Karlin KD. Electrochim. Acta. 2003; 48:4077.c) Willner I, Yan Y-M, Willner B, Tel-Vered R. Fuel Cells. 2009; 9:7.
16. a) Kadish KM, Frémond L, Shen J, Chen P, Ohkubo K, Fukuzumi S, Ojaimi ME, Gros CP, Barbe J-M, Guilard R. Inorg. Chem. 2009; 48:2571. [PubMed: 19215120] b) Kadish KM, Shen J, Frémond L, Chen P, El Ojaimi M, Chkounda M, Gros CP, Barbe J-M, Ohkubo K, Fukuzumi S, Guilard R. Inorg. Chem. 2008; 47:6726. [PubMed: 18582035]
17. Shook RL, Peterson SM, Greaves J, Moore C, Rheingold AL, Borovik AS. J. Am. Chem. Soc. 2011; 133:5810. [PubMed: 21425844]
18. a) Thorum MS, Yadav J, Gewirth AA. Angew. Chem. 2008; 121:171. *Angew. Chem. Int. Ed.***2008**, *48*, 165. b) Cracknell JA, Vincent KA, Armstrong FA. Chem. Rev. 2008; 108:2439. [PubMed: 18620369] c) Thorseth MA, Letko CS, Rauchfuss TB, Gewirth AA. Inorg. Chem. 2011; 50:6158. [PubMed: 21627090] d) McCrory CCL, Devadoss A, Ottenwaelder X, Lowe RD, Stack TDP, Chidsey CED. J. Am. Chem. Soc. 2011; 133:3696. [PubMed: 21366244]
19. Rolff M, Schottenheim J, Decker H, Tuczek F. Chem. Soc. Rev. 2011; 40:4077. [PubMed: 21416076]
20. Halfen JA, Mahapatra S, Wilkinson EC, Kaderli S, Young VG, Que L Jr, Zuberbühler AD Jr, Tolman WB. Science. 1996; 271:1397. [PubMed: 8596910]
21. a) Tolman WB. Acc. Chem. Res. 1997; 30:227.b) Lewis EA, Tolman WB. Chem. Rev. 2004; 104:1047. [PubMed: 14871149]
22. a) Itoh S, Fukuzumi S. Acc. Chem. Res. 2007; 40:592. [PubMed: 17461541] b) Itoh S, Fukuzumi S. Bull. Chem. Soc. Jpn. 2002; 75:2081.
23. a) Osako T, Ohkubo K, Taki M, Tachi Y, Fukuzumi S, Itoh S. J. Am. Chem. Soc. 2003; 125:11027. [PubMed: 12952484] b) Itoh S, Kumei H, Taki M, Nagatomo S, Kitagawa T, Fukuzumi S. J. Am. Chem. Soc. 2001; 123:6708. [PubMed: 11439064] c) Taki M, Itoh S, Fukuzumi S. J. Am. Chem. Soc. 2001; 123:6203. [PubMed: 11414865] d) Taki M, Teramae S, Nagatomo S, Tachi Y, Kitagawa T, Itoh S, Fukuzumi S. J. Am. Chem. Soc. 2002; 124:6367. [PubMed: 12033867]
24. a) Liang H-C, Zhang CX, Henson MJ, Sommer RD, Hatwell KR, Kaderli S, Zuberbühler AD, Rheingold AL, Solomon EI, Karlin KD. J. Am. Chem. Soc. 2002; 124:4170. [PubMed: 11960420] b) Mahadevan V, Henson MJ, Solomon EI, Stack TDP. J. Am. Chem. Soc. 2000; 122:10249.c) Kang P, Bobyr E, Dustman J, Hodgson KO, Hedman B, Solomon EI, Stack TDP. Inorg. Chem. 2010; 49:11030. [PubMed: 21028910] d) Hatcher LQ, Karlin KD. J. Biol. Inorg. Chem. 2004; 9:669. [PubMed: 15311336]
25. a) Thyagarajan S, Murthy NN, Sarjeant AAN, Karlin KD, Rokita SE. J. Am. Chem. Soc. 2006; 128:7003. [PubMed: 16719480] b) Karlin KD, Tyeklár Z, Farooq A, Haka MS, Ghosh P, Cruse RW, Gultneh Y, Hayes JC, Toscano PJ, Zubieta J. Inorg. Chem. 1992; 31:1436.
26. Lucas HR, Li L, Sarjeant AAN, Vance MA, Solomon EI, Karlin KD. J. Am. Chem. Soc. 2009; 131:3230. [PubMed: 19216527]
27. The activation entropy of electron transfer becomes negative when the electron transfer occurs via an intermediate; see: Fukuzumi S, Endo Y, Imahori H. J. Am. Chem. Soc. 2002; 124:10974. [PubMed: 12224933]

28. Addison, AW. Copper Coordination Chemistry: Biochemical, Inorganic Perspectives. Karlin, KD.; Zubieta, J., editors. New York: Adenine Press; 1983. p. 111
29. a) Su C-Y, Liao S, Wanner M, Fiedler J, Zhang C, Kang B-S, Kaim W. Dalton Trans. 2003:189. [PubMed: 15356712] b) Addison AW. Inorg. Chim. Acta. 1989; 162:217.c) Rybak-Akimova EV, Nazarenko AY, Chen L, Krieger PW, Herrera AM, Tarasov VV, Robinson PD. Inorg. Chim. Acta. 2001; 324:1.
30. a) Solomon EI, Baldwin MJ, Lowery MDH. Chem. Rev. 1992; 92:521.b) Hathaway, BJ. Comprehensive Coordination Chemistry, Vol. 5. Wilkinson, G., editor. Oxford: Pergamon; 1987. p. 533
31. For the E_{ox} values of ferrocene derivative, see: a) Lee Y-M, Kotani H, Suenobu T, Nam W, Fukuzumi S. J. Am. Chem. Soc. 2008; 130:434. [PubMed: 18085783] b) Fukuzumi S, Kotani H, Prokop KA, Goldberg DP. J. Am. Chem. Soc. 2011; 133:1859. c) Fukuzumi S, Kotani H, Suenobu T, Hong Y-M, Lee S, Nam W. Chem. Eur. J. 2010; 16:354. [PubMed: 19937616] d) Comba P, Fukuzumi S, Kotani H, Wunderlich S. Angew. Chem. 2010; 122:2679. *Angew. Chem. Int. Ed.* **2010**, *49*, 2622.
32. The E_{ox} values of ferrocene derivatives in acetone are virtually the same as those in MeCN; see: Noviandri I, Brown KN, Fleming DS, Gulyas PT, Lay PA, Masters AF, Phillips L. J. Phys. Chem. B. 1999; 103:6713.
33. The O_2 concentration in an O_2-saturated acetone solution (11 mM) was determined by the spectroscopic titration for the photooxidation of 10-methyl-9,10-dihydroacridine by O_2; see: Fukuzumi S, Ishikawa M, Tanaka T. J. Chem. Soc. Perkin Trans. 2. 1989:1037.
34. When the catalyst concentration of **1** (010 mM) was reduced to 0.020 mM, the non-catalytic formation of Fc^{*+} was not completely negligible. Nevertheless, four equivalents of Fc^{*+} were produced catalytically.
35. a) Mair RD, Graupner AJ. Anal. Chem. 1964; 36:194.b) Fukuzumi S, Kuroda S, Tanaka T. J. Am. Chem. Soc. 1985; 107:3020.
36. a) Marcus RA. Angew. Chem. 1993; 105:1161. *Angew. Chem. Int. Ed. Engl.***1993**, *32*, 1111. b) Marcus RA. Annu. Rev. Phys. Chem. 1964; 15:155.
37. Ohkubo K, Garcia R, Sintic PJ, Khoury T, Crossley MJ, Kadish KM, Fukuzumi S. Chem. Eur. J. 2009; 15:10493. [PubMed: 19711386]
38. Yang ES, Chan M-S, Wahl AC. J. Phys. Chem. 1980; 84:3094.
39. In the presence of large excess of TFA, however, the yield of formation of **3** becomes smaller because of the protonation of **3** (Figure S3 in the Supporting Information).
40. a) Chaka G, Bakac A. Dalton Trans. 2009:318. [PubMed: 19089013] b) Rosokha SV, Kochi JK. J. Am. Chem. Soc. 2007; 129:3683. [PubMed: 17338527]
41. Pidcock E, Obias HV, Abe M, Liang H-C, Karlin KD, Solomon EI. J. Am. Chem. Soc. 1999; 121:1299.
42. The ΔS_0 value may be negative because of the larger solvation of the more polarized bis-μ-oxo intermediate ($Cu^{III}(O^{2-})_2Cu^{III}$) as compared with that of the peroxo complex ($Cu^{II}(O_2^{2-})Cu^{II}$).
43. Armarego, WLF.; Chai, CLL. Purification of Laboratory Chemicals, 5th ed. Amsterdam: Butterworth-Heinemann; 2003.
44. Sheldrick, GM. SHELXTL/PC Version 6.12 for Windows XP. Madison, Wisconsin, USA: Bruker AXS Inc.; 2001.
45. Mann, CK.; Barnes, KK. Electrochemical Reactions in Nonaqueous Systems. New York: Marcel Dekker; 1990.

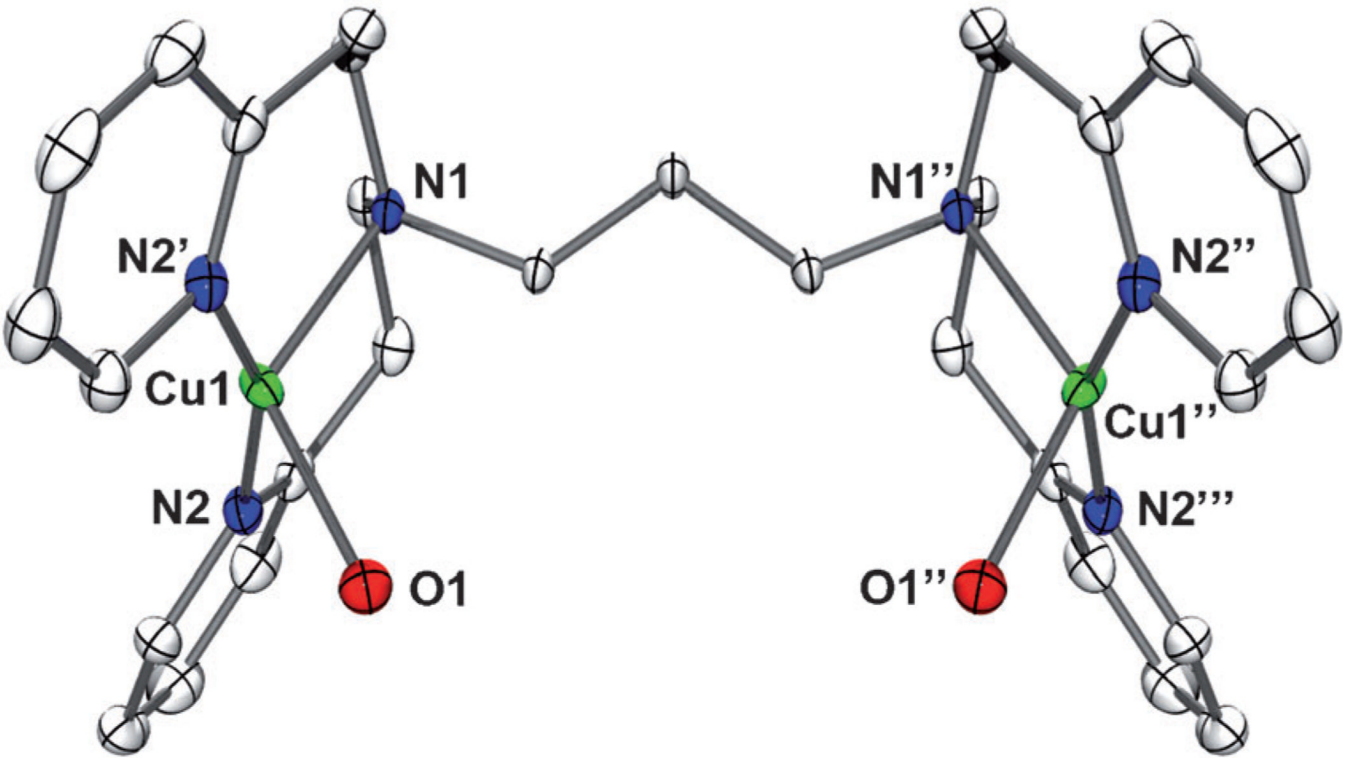

Figure 1.
X-ray crystal structure of $[Cu^{II}_2(N3)(H_2O)_2]^{4+}$ moiety in **1** with thermal ellipsoids drawn at the 30% probability level. Hydrogen atoms are omitted for clarity.

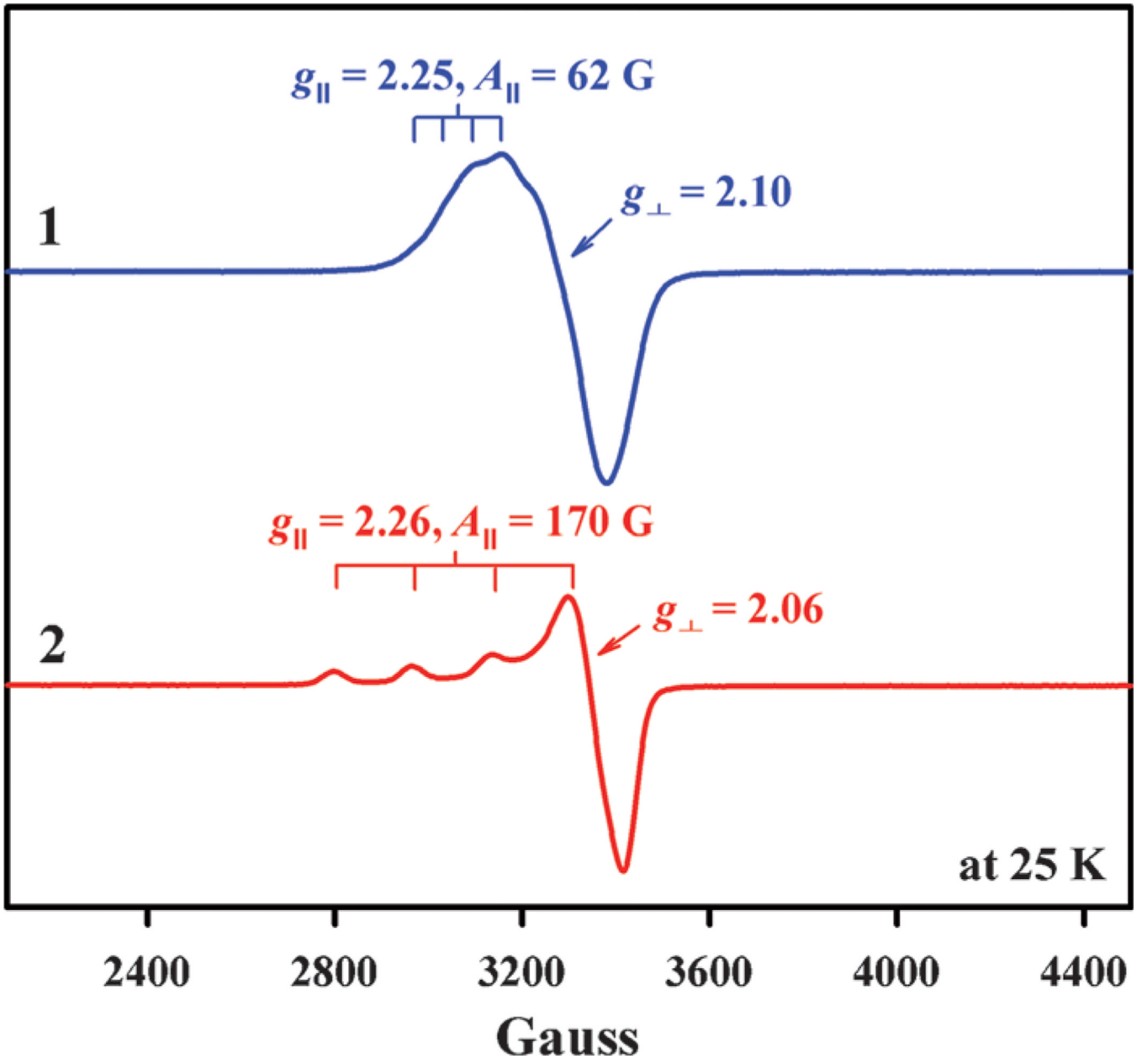

Figure 2.
X-band EPR spectra of $[Cu^{II}_2(N3)(H_2O)_2](ClO_4)_4$ (blue line, 1 mM) and $[Cu^{II}(BzPY1)(EtOH)](ClO_4)_2$ (red line, 1 mM) in acetone recorded at 25 K.

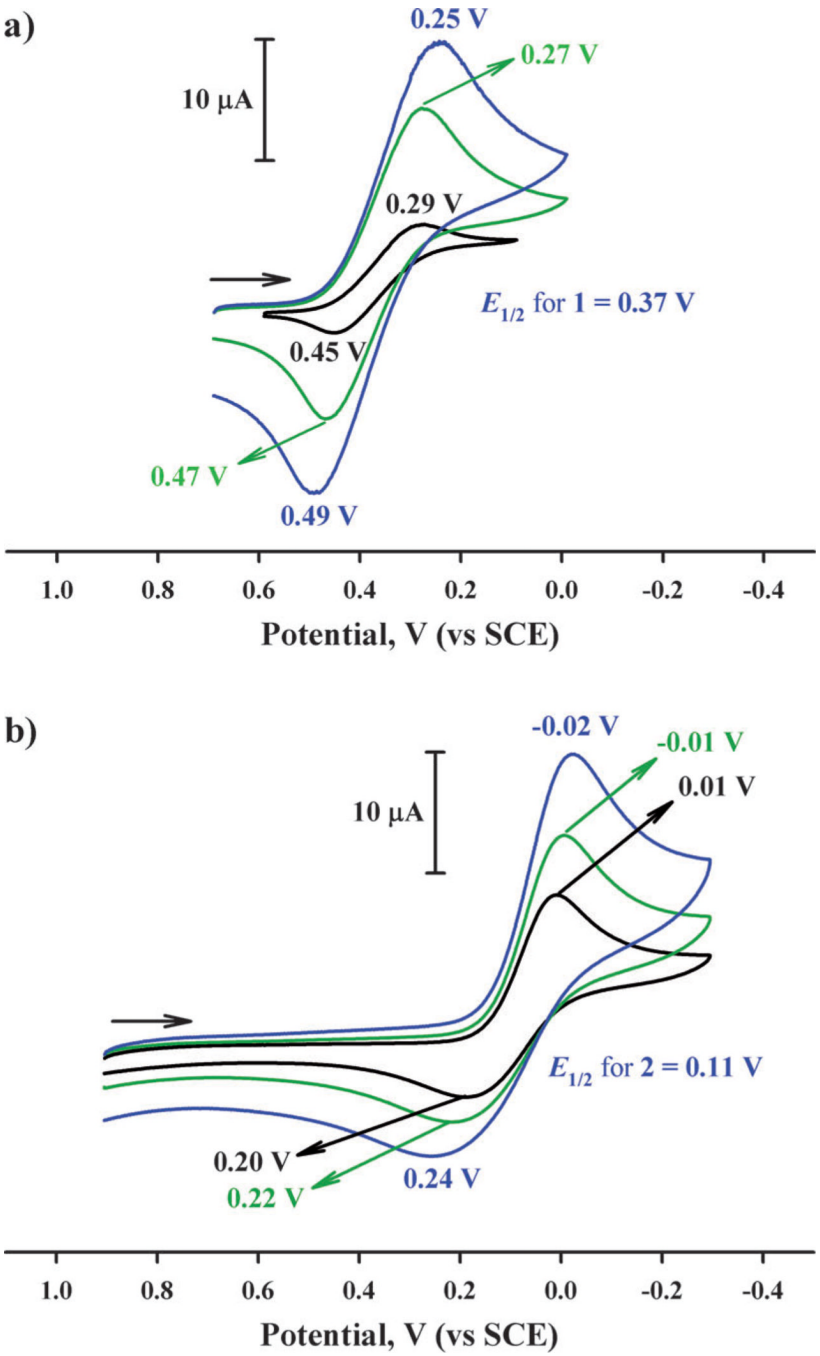

Figure 3.

Cyclic voltammograms of a) **1** (1.0 mM) and b) **2** (1.0 mM) in deaerated acetone containing $TBAPF_6$ (0.10 M) with a Pt working electrode at 298 K. The scan rates were 0.03 (black line), 0.2 (green line) and 0.4 V s^{-1} (blue line) for **1** and 0.1 (black line), 0.2 (green line) and 0.4 V s^{-1} (blue line) for **2**, respectively.

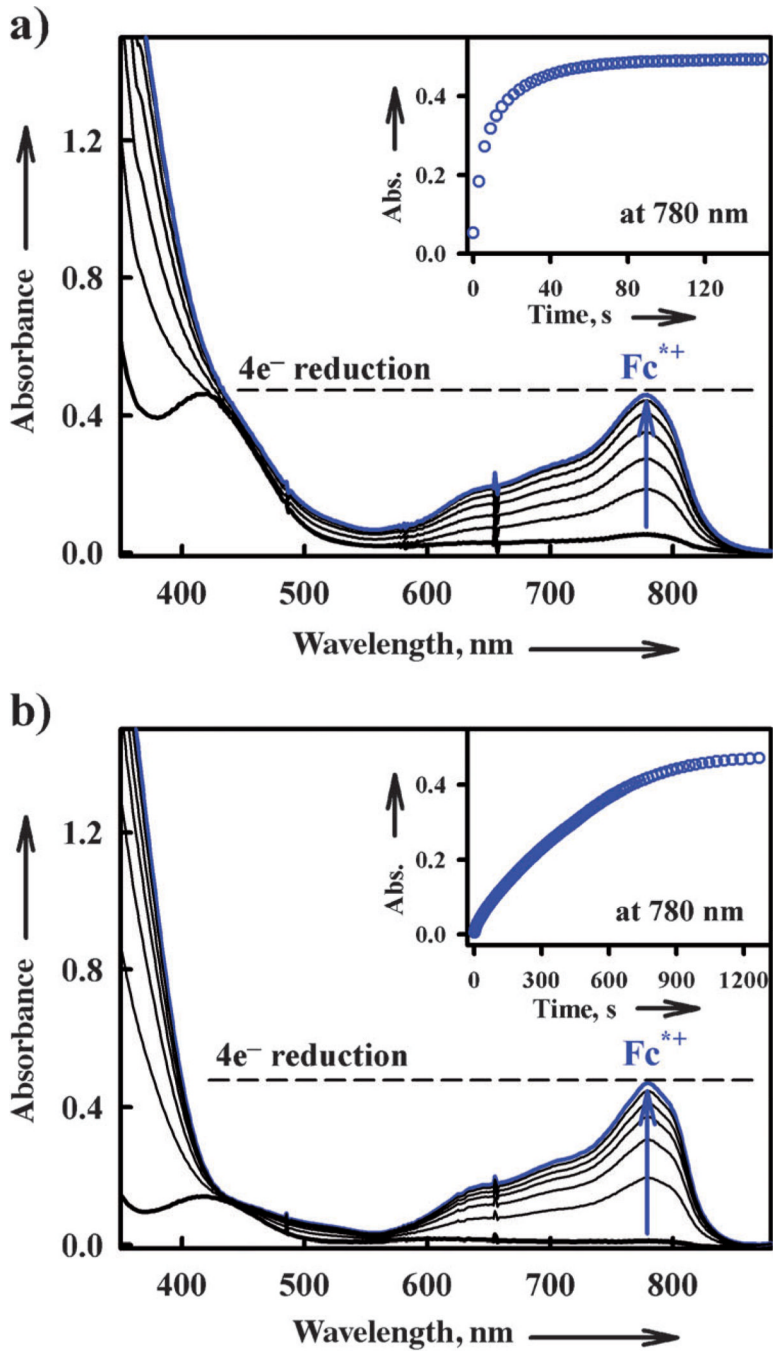

Figure 4.

UV/Vis spectral changes observed in the four-electron reduction of O_2 (0.22 mM) by Fc* (a) 3.0 mM at 298 K and b) 1.0 mM at 253 K) with TFA (10 mM) catalyzed by a) **1** (0.10 mM) and b) **2** (0.10 mM) in acetone. Inset shows the time profile of the absorbance at 780 nm due to Fc^{*+}.

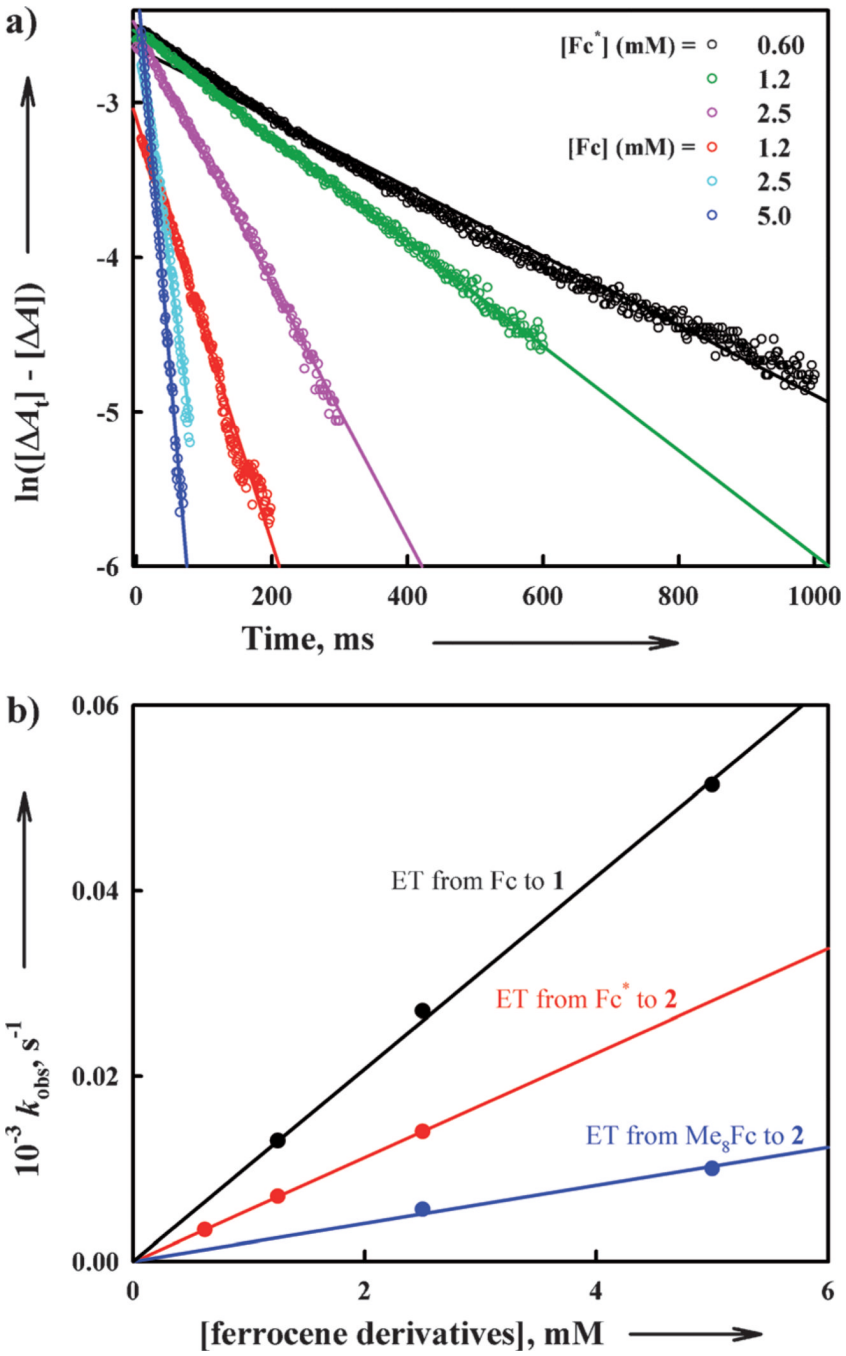

Figure 5.

a) First-order plots of electron transfer from Fc to **1** (red, cyan, and blue lines) and from Fc* to **2** (black, green and pink lines) in acetone at 298 K. b) Plots of the pseudo-first-order rate constants (k_{obs}) of electron transfer from ferrocene derivatives to **1** and **2** in acetone versus concentrations of ferrocene derivatives to determine the k_{et1} values at 298 K.

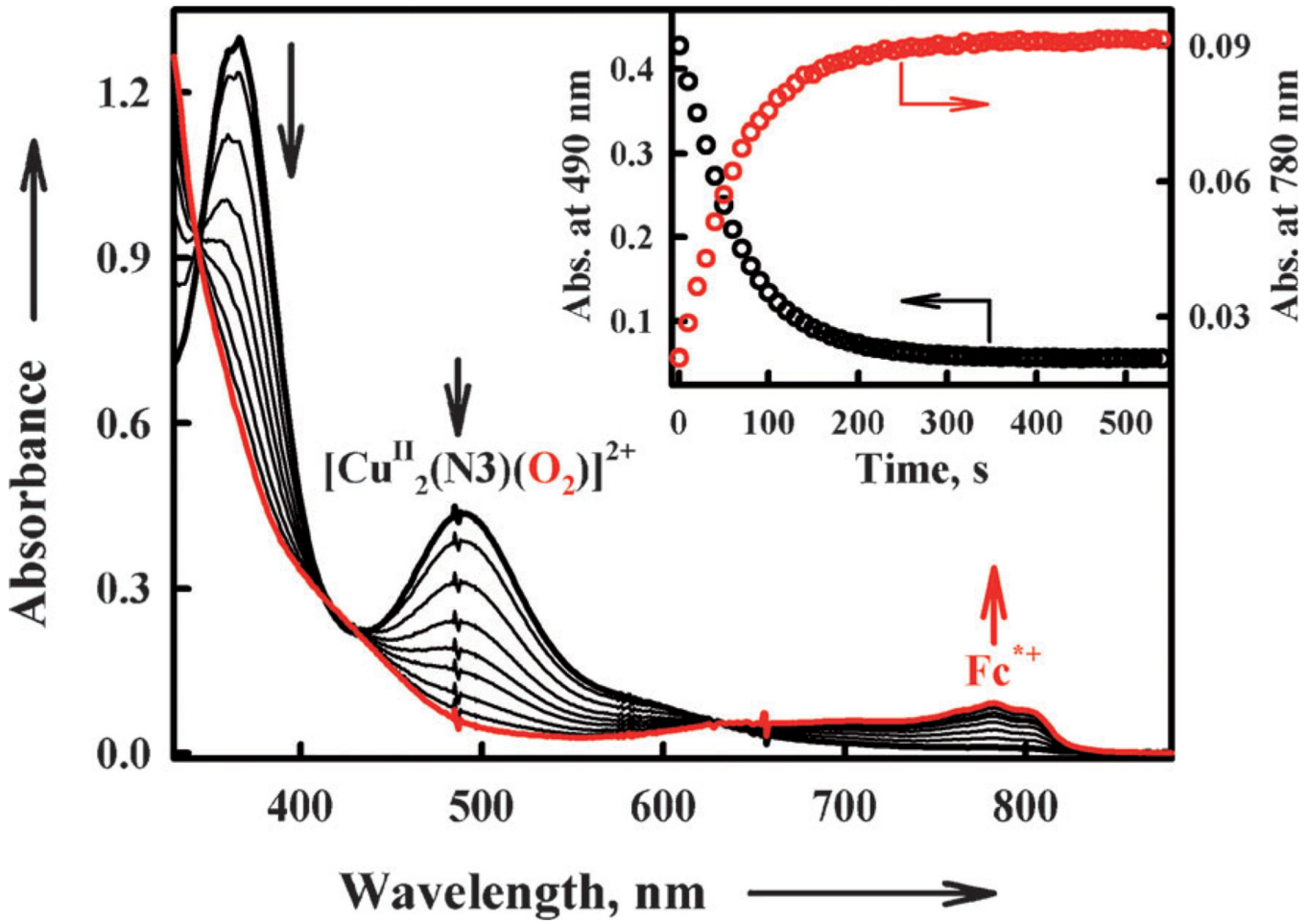

Figure 6.

Formation of the η^2:η^2-peroxo complex **3** (λ_{max} = 490 nm) in the reaction of $[Cu^{I}_2(N3)]^{2+}$ (0.10 mM) with O_2 in the presence of Fc* (0.80 mM) in acetone at 193 K. The inset shows the time profiles of the absorbance at 490 nm (black circles) and 780 nm (red circles) due to **3** and Fc^{*+}, respectively.

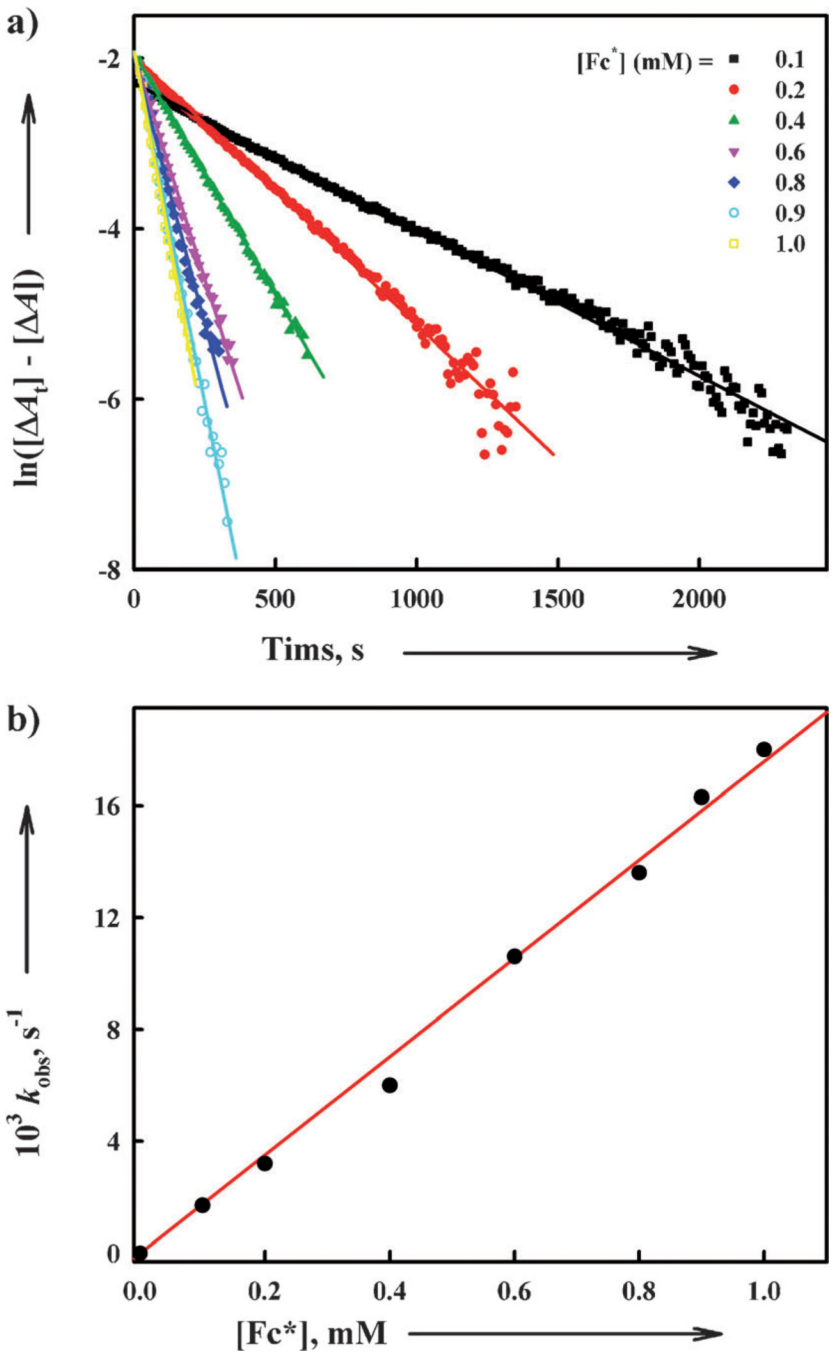

Figure 7.

a) First-order plots of electron transfer from Fc* to **3** in acetone at 193 K. b) Plot of the pseudo-first order rate constant (k_{obs}) of electron transfer from Fc* to **3** in acetone at 193 K versus Fc* concentration to determine the k_{et2} value.

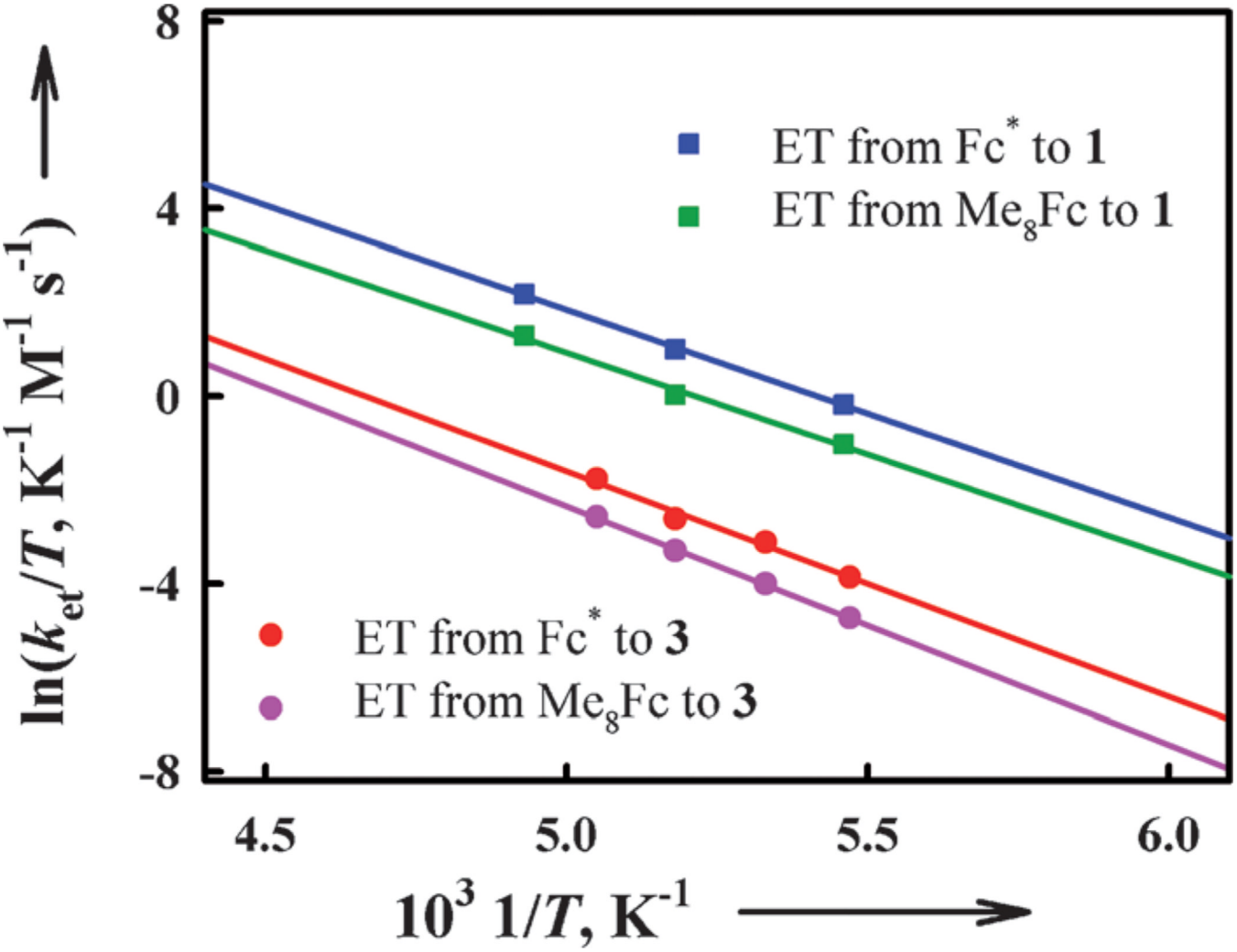

Figure 8.
Eyring plots of the rate constants (k_{et1} and k_{et2}) of electron transfer from Fc* and Me_8Fc to **1** and **3** in acetone.

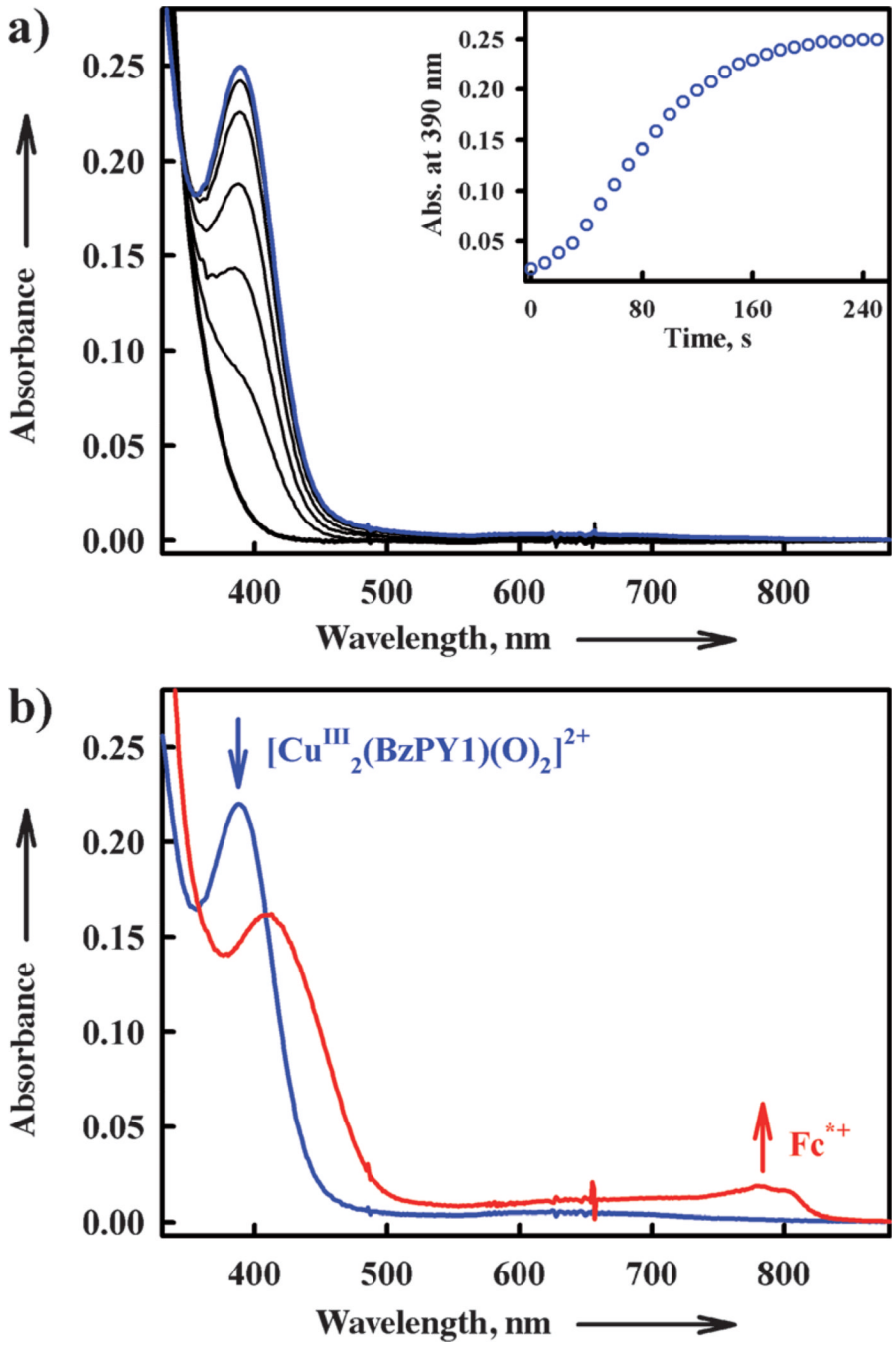

Figure 9.

a) Formation of the bis-μ-oxo complex **4** (λ_{max} = 390 nm) in the reaction of $[Cu^{I}(BzPY1)(CH_3CN)]^+$ (0.10 mM) with O_2 in acetone at 193 K. b) Formation of Fc^{*+} by addition of Fc* (0.70 mM) to the bis-μ-oxo complex generated. The reaction occurred upon mixing.

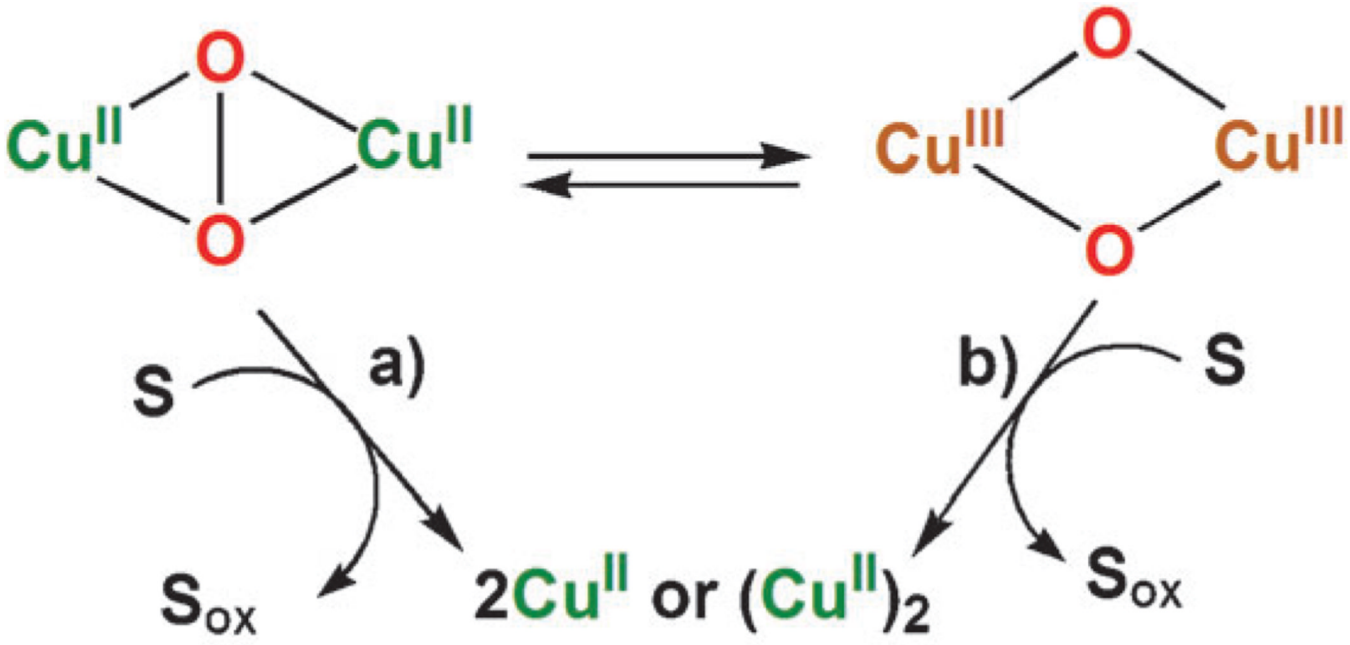

Scheme 1.

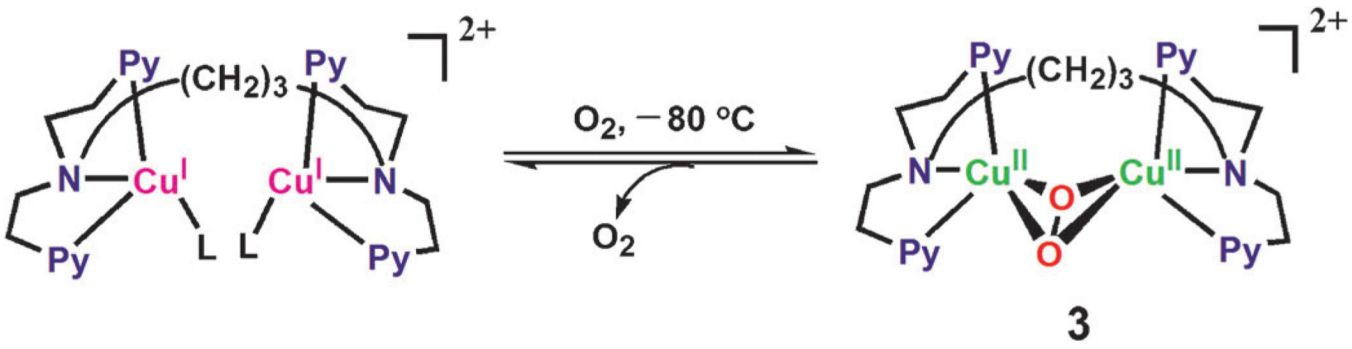

Scheme 2.

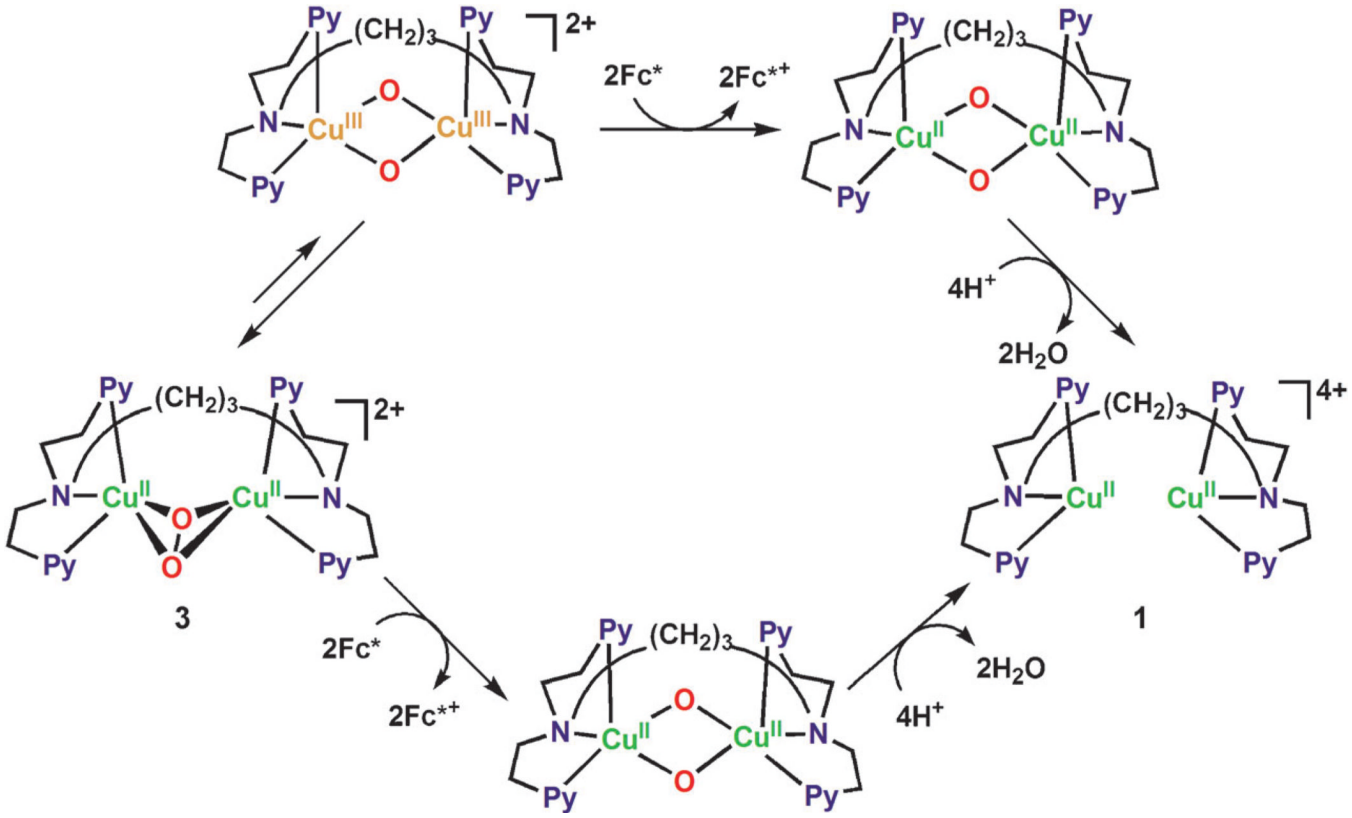

Scheme 3.

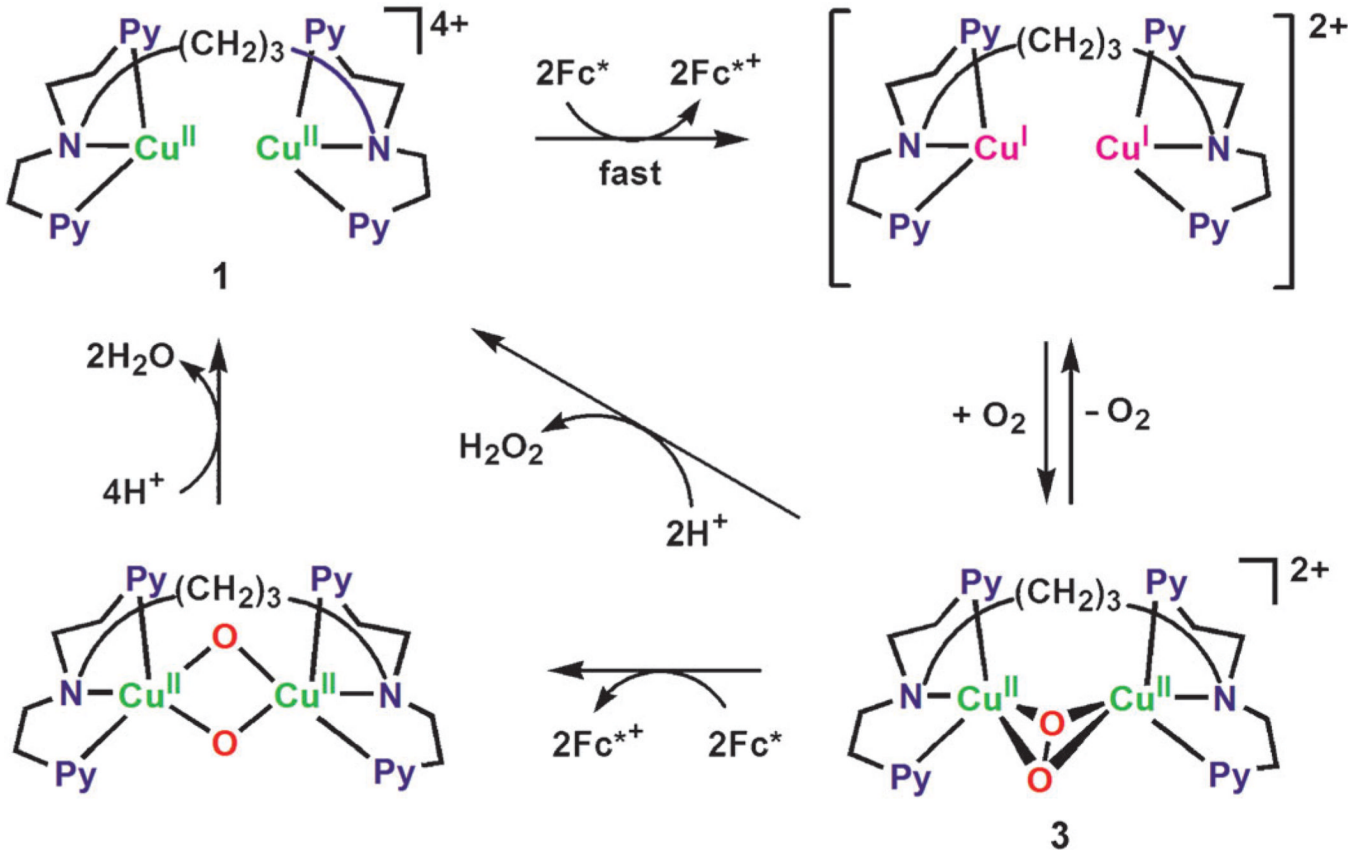

Scheme 4.

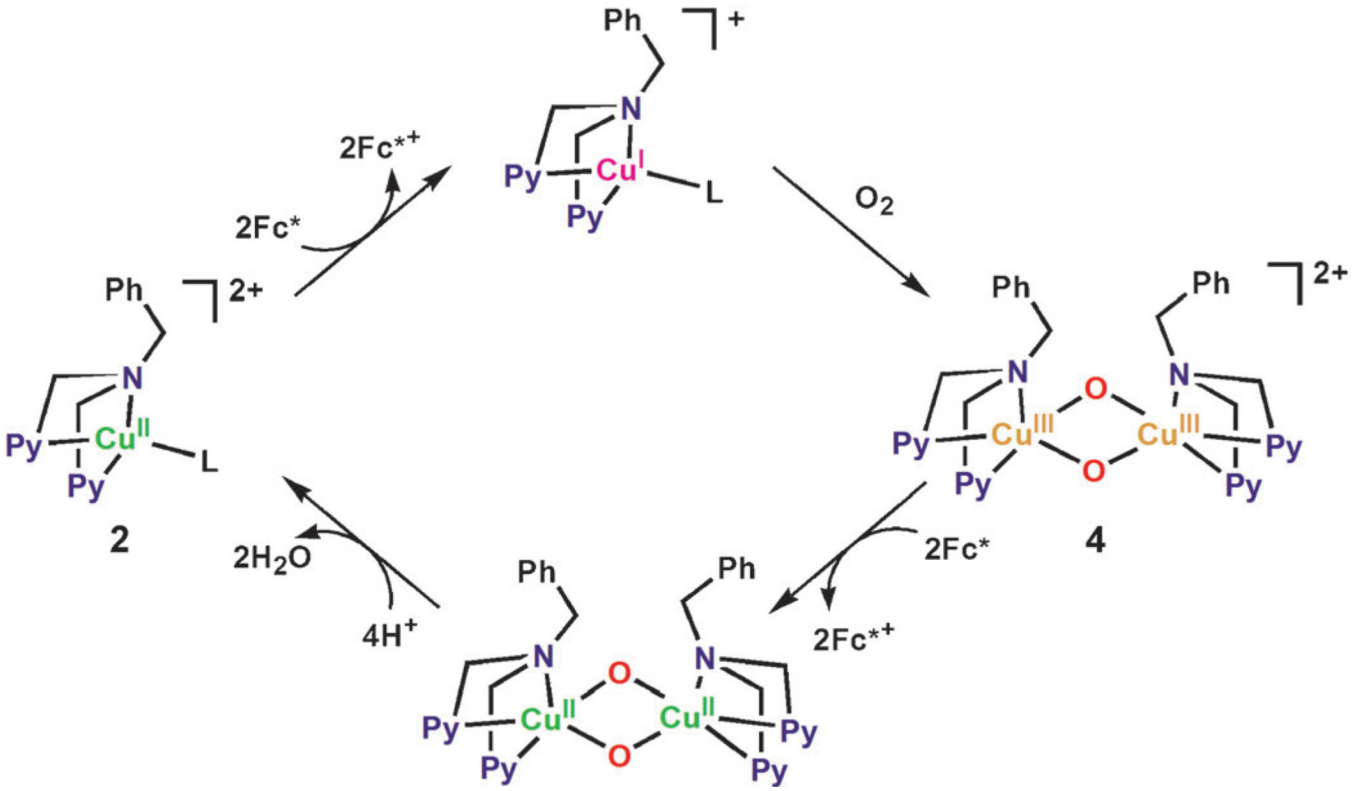

Scheme 5.

Table 1

One-electron oxidation potentials (E_{ox}) of ferrocene derivatives, rate constants (k_{et1}) of electron transfer from ferrocene derivatives to **1** and **2** in acetone at 298 K.

Ferrocene derivatives	E_{ox} **[V (vs. SCE)]**	k_{et1} **[M^{-1} s^{-1}]**	
		1	**2**
Fc*	−0.08	*[a]*	$(5.6\pm0.6) \times 10^3$
Me_8Fc	−0.04	*[a]*	$(1.8\pm0.3) \times 10^3$
Me_2Fc	0.26	$(2.4\pm0.3) \times 10^5$	*[b]*
Fc	0.37	$(1.1\pm0.2) \times 10^4$	*[b]*

[a] Too fast to be determined.

[b] No reaction.

Table 2

Activation parameters of electron transfer from Fc* and Me_8Fc to **1** and **3** in acetone.

Activation parameter	1		3	
	Fc*	Me_8Fc	Fc*	Me_8Fc
$\Delta H^{\ddagger}$ [kcal mol^{-1}]	(8.7±0.2)	(8.5±0.2)	(9.6±0.3)	(10.3±0.3)
$\Delta S^{\ddagger}$ [cal K^{-1} mol^{-1}]	(0±2)	(−3±2)	(−3±2)	(−1±2)